International Journal of GEOMATE, Nov., 2024 Vol.27, Issue 123, pp.133-140
ISSN: 2186-2982 (P), 2186-2990 (O), Japan, DOI: https://doi.org/10.21660/2024.123.g13424
Geotechnique, Construction Materials and Environment

SEISMIC PERFORMANCE EVALUATION AND VULNERABILITY ANALYSIS OF PRESTRESSED CONCRETE BRIDGE IN PADANG PARIAMAN REGENCY, INDONESIA

*Fauzan[1], Prima Yane Putri[2], Zev Al Jauhari[3], Dani Iswara Sundari[4], and Geby Aryo Agista[5]

[1,4,5]Department of Civil Engineering, Faculty of Engineering, Universitas Andalas, Indonesia;
[2]Department of Civil Engineering, Faculty of Engineering, Universitas Negeri Padang, Indonesia;
[3]Graduate School of Engineering, Toyohashi University of Technology, Japan

*Corresponding Author, Received: 21 July 2023, Revised: 23 Sep. 2024, Accepted: 25 Sep. 2024

ABSTRACT: In recent years, major earthquakes have caused damage to infrastructure, especially bridge structures. The case of the Gaoliao Bridge collapse following the 6.9 magnitude earthquake in 2022 in Taiwan highlights the importance of conducting performance evaluations during maintenance periods, especially in earthquake-prone areas. Indonesia is located in the Pacific Ring of Fire zone, so earthquakes often occur in several regions of Indonesia, including West Sumatra Province. This study carried out seismic performance evaluations of a prestressed concrete bridge, the STA 6+200 bridge of the Trans Sumatra Toll Road Project, in Padang Pariaman Regency. Seismic performance evaluation of the prestressed concrete bridge was carried out using the finite element method (SAP2000 v21) in terms of the prestressed concrete beam's bending moment and shear capacity and deflection. In addition, vulnerability analysis using fragility curves was carried out to predict the level of damage to bridge structures due to earthquake loads. A fragility curve through dynamic response analysis of scaled nonlinear time histories (Incremental Dynamic Analysis) due to the Kobe, Imperial Valley, and Northridge earthquakes was developed using a log-normal distribution function. The results of the study show that the moment, shear, and deflection of the prestressed concrete bridge meet the Indonesian bridge permit code. Additionally, the results of the fragility curve show that the prestressed concrete bridge with a PGA value in bridge location of 0.481g has a 26% probability of experiencing slight damage, and there is no possibility of moderate, extensive, and complete damage, indicating that the prestressed concrete bridge structure is effective in ensuring structural safety and resilience.

Keywords: Earthquake, Prestressed Concrete Bridge, Bridge Performance, Vulnerability Analysis, Fragility Curve

1. INTRODUCTION

The Pacific Ring of Fire is a major region in the Pacific Ocean basin where earthquakes and volcanic eruptions frequently occur. It is a roughly 25,000-mile chain of volcanoes and seismically active sites that outline the Pacific Ocean [1]. Currently, earthquake disaster estimation and prediction are still difficult to achieve, especially in earthquake-prone areas in the Ring of Fire. In recent years, several major earthquakes have damaged infrastructure, especially bridge structures.

The Gaoliao Bridge in Taiwan is one case of a bridge structure failing against earthquake load in recent years, as shown in Fig. 1. On September 18, 2022, an earthquake with a local magnitude (ML) 6.8 struck the southern part of Longitudinal Valley in southeastern Taiwan, resulting in the collapse and damage of many engineering structures [2]. This highlights the importance of conducting performance evaluations during maintenance periods, particularly in earthquake-prone areas, to prevent collapse during an earthquake.

Recently, many seismic performance evaluations and vulnerability analyses of bridge structures have been carried out, such as seismic fragility assessment for a newly developed buried arch bridge [3], seismic vulnerability analysis of long span prestressed concrete continuous rigid frame bridge [4], fragility curves of RC bridges in México [5], fragility analysis of existing prestressed concrete bridges under traffic loads according to new Italian guidelines [6].

Fig. 1 The Gaoliao Bridge collapsed after a 6.9 M earthquake in Taiwan [2]

Indonesia is highly prone to earthquakes due to its location within the Pacific Ring of Fire. One of the regions in Indonesia that is prone to earthquakes is West Sumatra, so all structural planning must follow construction rules and applicable regulations in order to reduce the impact of damage and losses due to earthquakes. One of the bridge constructions in West Sumatra, namely the under-bridge STA 6+200 Trans Sumatra Toll Road Construction Project, Pekanbaru-Padang Section, Sicincin-Lubuk Alung-Padang Section, in Padang Pariaman Regency. The underbridge that crosses this national road is a type of prestressed concrete bridge, as shown in Fig. 2.

Fig. 2 Prestressed concrete bridge in Padang Pariaman Regency, Indonesia

The prestressed concrete bridge requires seismic performance evaluation and vulnerability analysis of the bridge to ensure that it does not collapse during an earthquake. In this study, seismic performance evaluations of a prestressed concrete bridge were carried out on the STA 6+200 bridge of the Trans Sumatra Toll Road Project. Seismic performance evaluation of the prestressed concrete bridge was carried out using the finite element method (SAP2000 v21) in terms of the prestressed beam's bending moment and shear capacity and deflection. In addition, vulnerability analysis using fragility curves was carried out to predict the level of damage to bridge structures due to earthquake loads.

2. RESEARCH SIGNIFICANCE

The study focuses on seismic performance evaluation of a prestressed concrete bridge and vulnerability analysis using fragility curves to ensure structural safety and resilience. It also aims to validate the capacity of bridge structures to withstand operational loads according to current Indonesian bridge regulations. Additionally, the fragility curve developed can forecast potential levels of damage to the bridge, serving as a preventive measure to ensure it remains stable and avoids collapse during an earthquake. The results of the study are expected to contribute to the basic idea of design performance evaluation of prestressed concrete bridges against earthquake loads.

3. STRUCTURAL ANALYSIS

3.1 Bridge Existing Data

The prestressed concrete bridge has two abutments and three pairs of piers. The total length of the bridge, including approaches from abutment to abutment, is 160.1 m. The width of the bridge is 12.7 m. Table 1 shows a description of the bridge's existing data properties.

Table 1 Bridge existing data

Name	Data
Bridge structure	Prestr. concrete bridges
Length	160.1 m
Bridge configuration	40.8–30.8–40.8–40.8 m
Width	12.700 m
Steel grade	BJTD 40
Types of foundation	Steel pipe D800 mm

3.2 Structural Modeling

The structural elements modelled include longitudinal girders (girder beams), transverse girders (diaphragms), floor plates, pier heads, piers, abutments, and pile caps. The structure is modelled using a finite element method (SAP2000 v21) computer program [7], as shown in Fig. 3.

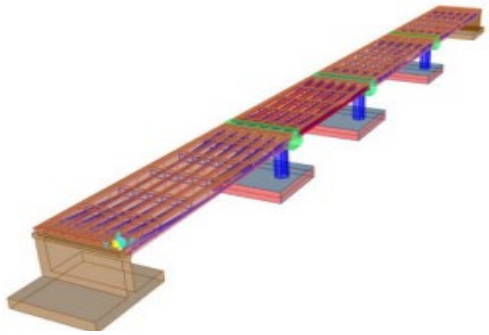

Fig. 3 Prestressed concrete bridge 3D modeling

3.3 Load Analysis

3.3.1 Dead Load

The dead load represents the combined weight of all structural and non-structural components (additional) of the prestressed concrete bridge. It is determined by multiplying the material weight by the dimensions of the structural elements. Additional dead load consists of the weight of non-structural materials added to the bridge, and its loading value can change during the life of the bridge, as shown in Table 2. The guidelines for dead load are outlined in SNI 1725:2016 [8].

Table 2 Additional dead load

Additional load	Value	Unit
Barrier	1311.650	kN
Puddle	0.490	kN/m^2

3.3.2 Live load

The live load is derived from vehicle loads specified by SNI 1725:2016 [8]. The calculated live load comprises evenly distributed loads and point loads on girder load assignment. Details of the live load calculation are provided in Table 3.

Table 3 Live load

Live load	Value	Unit
Uniformly distributed load (l=40.8 m)	7.809	kPa
Uniformly distributed load (l=30.8 m)	8.883	kPa
Point load	68.600	kN/m

3.3.3 Wind load

The wind load on the structure is considered to be uniformly distributed across the exposed section facing the wind. The applied wind load is quantified at 4.4 kN/mm [8].

3.3.4 Earthquake load

The time history of earthquake loads based on SNI 2833:2016 Earthquake Resistance Planning Standard for Bridge [9] was used in the analysis. The specific earthquake acceleration values utilized as shown in Table 4.

Table 4 Earthquake acceleration data

Earthquake	Value	Unit
Kobe-X	0.580	g
Kobe-Y	0.560	g
Imperial Valley-X	0.550	g
Imperial Valley-Y	0.590	g
Northridge-X	0.620	g
Northridge-Y	0.460	g

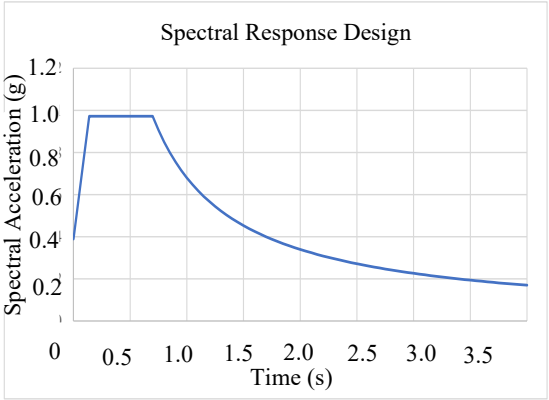

Fig. 4 Spectral response design of Padang Pariaman Regency

The earthquake acceleration was fine-tuned to match the spectral response of Padang Pariaman Regency, ensuring compatibility with the structure's location. The peak acceleration of bedrock (PGA) location of the existing bridge is 0.481 g, with Ss of 1.459 g and S1 of 0.600 g. Figure 4 shows a graph illustrating the spectral response of Padang Pariaman Regency.

The earthquake acceleration data was adjusted to match the spectral response using the finite element method with the SAP2000 v21 computer program. The adjusted data was then input into the load case as an earthquake load. Figure 5 presents the results of the adjustment between the earthquake acceleration data and the spectral response of Padang Pariaman Regency.

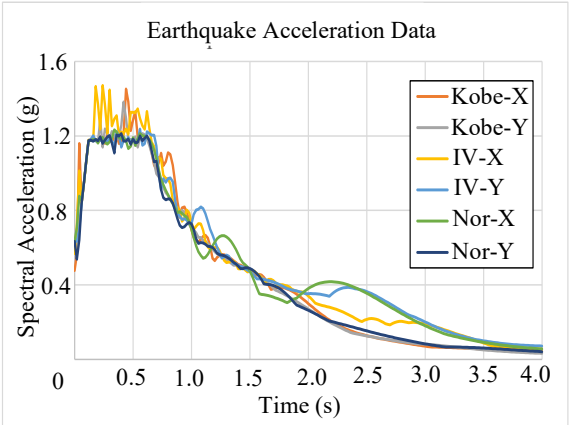

Fig. 5 Earthquake acceleration adjustment results

3.3.5 Load combination

In this study, the load combination was calculated according to the guidelines outlined in SNI 1725:2016 regarding loading for bridges. These combinations are categorized into serviceability combinations, which are employed to compute stress and deflection in the bridge structure, and ultimate strength combinations, utilized to assess the stability of the bridge against bridge structural response. Tables 5 and 6 provide detailed descriptions of each combination.

Table 5 Service load combination

Load Combination Limit State	Load factors
Service I	MS + MA + PR + TD + 0.3 EWS
Service II	MS + MA + PR + 1.3 TD
Service III	MS + MA +PR + 0.8 TD
Service IV	MS + MA + PR + 0.7 EWS
Service Extreme	MS + MA + PR + 0.5 TD + EQ

According to Tables 5 and 6, MS is dead load due to structural members and other permanent fixtures; MA is dead load due to non-structural attachments;

PR is Live load, which includes the loads from occupancy or usage; TD is Thermal differential load, which accounts for stresses due to temperature changes; EWS is Earthquake Wind Seismic load, which is a combination of loads due to seismic activities and wind forces; EQ is Earthquake load, which specifically accounts for loads due to seismic activity.

Table 6 Strength load combination

Load Combination Limit State	Load factors
Strength I	1.2 MS + 1.4 MA + PR + 1.8 TD
Strength II	1.2 MS + 1.4 MA + PR + 1.4 TD
Strength III	1.2 MS + 1.4 MA + PR + 1.4 EWS
Strength IV	1.2 MS + 1.4 MA + PR
Strength V	1.2 MS + 1.4 MA + PR + 0.4 EWS
Extreme Event I	1.2 MS + 1.4 MA + PR + 0.5 TD + EQ

4. RESULTS AND DISCUSSION

4.1 Prestressed Concrete Bridge Capacity

In this study, analysis of prestressed concrete bridge capacity is employed to ensure that the concrete remains in compression or within allowable tensile stress limits under service load conditions [10-12].

4.1.1 Moment capacity of prestressed concrete girder

- Girder bridge 40.8 m
  Width (b) : 800 mm
  Height (h) : 2100 mm
  Tendon area (A_{ps}) : 10260.826 mm^2
  Strand tensile strength (f_{pu}) : 1840 MPa
  Compressive strength (fc') : 50 MPa
- Girder bridge 30.8 m
  Width (b) : 800 mm
  Height (h) : 1700 mm
  Tendon area (A_{ps}) : 7220.582 mm^2
  Strand tensile strength (f_{pu}) : 1840 MPa
  Compressive strength (fc') : 50 MPa

The calculation of moment capacity is expressed by the following Eq. (1):

$$M_U = \phi \left[A_{ps} \,.\, f_{ps} \,.\, \left(d - \frac{a}{2} \right) \right] \quad (1)$$

where A_{ps} is tendon area; f_{ps} is steel stress; d is diameter of tendon. Tables 7 and 8 show the calculation result of the moment capacity for each length girder bridge. The moment capacity result of the girders (l = 40.8 m and 30.8 m) shows that the bridge can withstand the working loads and meet the requirements of the current Indonesian bridge standard.

Table 7 Moment capacity of 40.8 m girder bridge

Load Comb.	Assess. Area	Moment (kN-m)		Mn ≥ Mu
		Ultimate (Mu)	Capacity (Mn)	
Strength I	Interior	5208.774	25392.011	OK
	Exterior	4921.480	25392.011	OK
Strength II	Interior	4861.177	25392.011	OK
	Exterior	4482.780	25392.011	OK
Strength III	Interior	10807.43	25392.011	OK
	Exterior	12514.00	25392.011	OK
Strength IV	Interior	4282.573	25392.011	OK
	Exterior	3711.850	25392.011	OK
Strength V	Interior	4622.223	25392.011	OK
	Exterior	4285.410	25392.011	OK
Extreme Event I	Interior	4360.653	25392.011	OK
	Exterior	3819.687	25392.011	OK

Table 8 Moment capacity of 30.8 m girder bridge

Load Comb.	Assess. Area	Moment (kN-m)		Mn ≥ Mu
		Ultimate (Mu)	Capacity (Mn)	
Strength I	Interior	1929.921	15144.831	OK
	Exterior	2465.692	15144.831	OK
Strength II	Interior	1871.101	15144.831	OK
	Exterior	2409.883	15144.831	OK
Strength III	Interior	4221.554	15144.831	OK
	Exterior	6282.051	15144.831	OK
Strength IV	Interior	1787.198	15144.831	OK
	Exterior	2321.900	15144.831	OK
Strength V	Interior	2082.201	15144.831	OK
	Exterior	2856.898	15144.831	OK
Extreme Event I	Interior	1801.772	15144.831	OK
	Exterior	2343.998	15144.831	OK

4.1.2 Shear capacity of prestressed concrete girder

- Girder bridge 40.8 m
  Length (L) : 40.8 m
  Review point (1/4L) : 10.4 m
  Moment ultimate (Mu) : 9970.4 kN-m
  Shear ultimate (Vu) : 525.053 kN
  Yield stress (fy) : 400 MPa
  Compressive strength (fc') : 50 MPa
  Thick web midspan area (bw) : 200 mm
  Area of reinforcement (Av) : 132.732 mm^2
  Distance of stirrup (midspan) : 100 mm
  Effective girder height (d) : 1930 mm
- Girder bridge 30.8 m
  Length (L) : 30.8 m
  Review point (1/4L) : 7.7 m
  Moment ultimate (Mu) : 5406.878 kN-m
  Shear ultimate (Vu) : 462.405 kN
  Yield stress (fy) : 400 MPa
  Compressive strength (fc') : 50 MPa
  Thick web midspan area (bw) : 200 mm
  Area of reinforcement (Av) : 132.732 mm^2
  Distance of stirrup (midspan) : 100 mm
  Effective girder height (d) : 1580 mm

The shear capacity of the prestressed concrete girder was calculated using Eq. (2):

$$V_n = \phi(V_s + V_c) \quad (1)$$

Referring to Eq. (2), the moment capacity values for each girder are obtained and presented in Tables 9 and 10. Based on the calculations, the shear capacity meets the bridge requirements in the bridge standard.

Table 9 Shear capacity of 40.8 m length girder

Load Comb.	Assess. Area	Shear (kN)		Vu ≤ Vn
		Shear (Vu)	Capacity (Vn)	
Strength I	Interior	491.547	1116.521	OK
	Exterior	420.251	1116.521	OK
Strength II	Interior	491.020	1116.521	OK
	Exterior	407.488	1116.521	OK
Strength III	Interior	801.766	1116.521	OK
	Exterior	620.634	1116.521	OK
Strength IV	Interior	490.212	1116.521	OK
	Exterior	387.129	1116.521	OK
Strength V	Interior	518.685	1116.521	OK
	Exterior	411.192	1116.521	OK
Extreme Event I	Interior	491.137	1116.521	OK
	Exterior	391.402	1116.521	OK

Table 10 Shear capacity of 30.8 m length girder

Load Comb.	Assess. Area	Shear (kN)		Vu ≤ Vn
		Shear (Vu)	Capacity (Vn)	
Strength I	Interior	710.390	1053.412	OK
	Exterior	645.116	1053.412	OK
Strength II	Interior	655.768	1053.412	OK
	Exterior	606.445	1053.412	OK
Strength III	Interior	751.801	1053.412	OK
	Exterior	542.885	1053.412	OK
Strength IV	Interior	561.931	1053.412	OK
	Exterior	541.907	1053.412	OK
Strength V	Interior	425.882	1053.412	OK
	Exterior	334.396	1053.412	OK
Extreme Event I	Interior	637.839	1053.412	OK
	Exterior	568.975	1053.412	OK

4.1.3 Deflection

Deflection is a crucial aspect examined to evaluate the performance of the under-bridge structure. The allowable deflection is determined using the following Eq. (3):

$$\delta_{allowable} = \frac{L}{300} \quad (3)$$

The result of deflection from SAP2000 v21 (δ_{max}) was compared to those from Eq. (3) (δ_{limit}), as shown in Tables 11 and 12. From these tables, it is seen that the deflection of prestressed concrete bridge meets the requirements of Indonesian bridge codes ($\delta_{max} \leq \delta_{limit}$).

Table 11 Deflection of 40.8 prestressed beam

Load Comb.	Assess. Area	Deflection (m)		$\delta_{max} \leq \delta_{limit}$
		δ_{max}	δ_{limit}	
Service I	Interior	4.53×10^{-3}	0.136	OK
	Exterior	9.90×10^{-3}	0.136	OK
Service II	Interior	1.43×10^{-3}	0.136	OK
	Exterior	1.52×10^{-3}	0.136	OK
Service III	Interior	1.42×10^{-3}	0.136	OK
	Exterior	1.38×10^{-3}	0.136	OK
Service IV	Interior	1.01×10^{-2}	0.136	OK
	Exterior	2.29×10^{-2}	0.136	OK
Service extreme	Interior	1.45×10^{-3}	0.136	OK
	Exterior	1.52×10^{-3}	0.136	OK

Table 12 Deflection of 30.8 prestressed beam

Load Comb.	Assess. Area	Deflection (m)		$\delta_{max} \leq \delta_{limit}$
		δ_{max}	δ_{limit}	
Service I	Interior	3.79×10^{-3}	0.103	OK
	Exterior	6.96×10^{-3}	0.103	OK
Service II	Interior	3.93×10^{-3}	0.103	OK
	Exterior	1.98×10^{-3}	0.103	OK
Service III	Interior	3.62×10^{-3}	0.103	OK
	Exterior	1.30×10^{-3}	0.103	OK
Service IV	Interior	3.77×10^{-3}	0.103	OK
	Exterior	1.58×10^{-2}	0.103	OK
Service extreme	Interior	3.51×10^{-3}	0.103	OK
	Exterior	1.05×10^{-3}	0.103	OK

4.2 Development of Fragility Curves

In this study, vulnerability analysis using fragility curves was conducted to predict the level of damage to bridge structures due to seismic loads. The fragility curves were obtained through non-linear time history analysis and Incremental Dynamic Analysis (IDA), considering the Kobe, Imperial Valley, and Northridge earthquakes, and were developed using a log-normal distribution function.

4.2.1 Incremental Dynamic Analysis (IDA)

The parameter of the seismic fragility curve requires the maximum displacement of the prestressed concrete bridge, obtained from IDA and structural modeling responses using the finite element program SAP2000. IDA simulates earthquakes of varying intensities applied to the bridge structure model until collapse occurs.

IDA is utilized here to determine earthquake-induced displacements using a scale factor of 0.2 in the non-linear time history analysis. The acceleration data used in this analysis are from Kobe, Imperial Valley, and Northridge. The structural responses regarding displacement due to Incremental Dynamic Analysis are documented for both X and Y earthquake directions, as shown in Table 13. The evaluation point for determining the displacement due to seismic loads was focused on the top of Pier 1. These values will later be used to determine the level

of structural damage and the performance level of the bridge.

Table 13 Displacement due to earthquake

Name of Earthquake	Scale Factor	X-Direction (mm)	Y-Direction (mm)
Kobe	0.20	7.040	3.040
Kobe	0.40	21.780	4.500
Kobe	0.60	37.310	5.380
Kobe	0.80	57.150	6.150
Kobe	1.00	76.850	7.660
Kobe	1.20	96.480	9.760
Kobe	1.40	116.060	12.830
Kobe	1.60	135.620	15.920
Kobe	1.80	155.190	18.990
Kobe	2.00	174.770	22.070
Imperial Valley	0.20	8.420	3.470
Imperial Valley	0.40	24.240	4.770
Imperial Valley	0.60	41.170	6.050
Imperial Valley	0.80	58.800	7.010
Imperial Valley	1.00	76.460	9.800
Imperial Valley	1.20	94.650	12.360
Imperial Valley	1.40	112.850	15.190
Imperial Valley	1.60	131.060	18.200
Imperial Valley	1.80	142.960	21.110
Imperial Valley	2.00	167.440	23.800
Northridge	0.20	7.400	2.890
Northridge	0.40	19.490	5.570
Northridge	0.60	36.990	8.690
Northridge	0.80	55.320	11.630
Northridge	1.00	74.120	14.480
Northridge	1.20	93.270	17.230
Northridge	1.40	112.580	9.950
Northridge	1.60	131.980	22.670
Northridge	1.80	151.420	25.360
Northridge	2.00	170.890	28.050

The variation in displacement response is linked to the configuration of the bridge structure, with the transverse direction (Y-axis) identified as the strong axis, while the longitudinal direction (X-axis) is considered the weak axis of the bridge. Given that bridge damage is more prominent in the longitudinal direction, this study focuses on reviewing displacement in that direction as a reference for constructing a fragility curve, as shown in Table 14.

Structural damage measures are employed to determine damage levels, indicating the structure's performance against earthquakes. HAZUS categorizes damage levels into Slight, Moderate, Extensive, and Complete [10]. Meanwhile, performance levels can be established based on Bridge Design/Performance Parameters (NCHRP 440, 2013) [11], as illustrated in Table 15.

Table 14 Degree of structural damage

Earthquake	Scaled PGA	Max. Displ. (mm)	Drift (%)	Damage State
Kobe-X	0.12	7.040	0.10	Slight
Kobe-X	0.23	21.780	0.32	Slight
Kobe-X	0.35	37.310	0.55	Slight
Kobe-X	0.46	57.150	0.84	Slight
Kobe-X	0.58	76.850	1.13	Moderate
Kobe-X	0.70	96.480	1.41	Moderate
Kobe-X	0.81	116.060	1.70	Moderate
Kobe-X	0.93	135.620	1.99	Moderate
Kobe-X	1.04	155.190	2.27	Moderate
Kobe-X	1.16	174.770	2.56	Moderate
Imperial Valley-X	0.11	8.420	0.12	Slight
Imperial Valley-X	0.22	24.240	0.35	Slight
Imperial Valley-X	0.33	41.170	0.60	Slight
Imperial Valley-X	0.44	58.800	0.86	Slight
Imperial Valley-X	0.55	76.460	1.12	Moderate
Imperial Valley-X	0.66	94.650	1.39	Moderate
Imperial Valley-X	0.77	112.850	1.65	Moderate
Imperial Valley-X	0.88	131.060	1.92	Moderate
Imperial Valley-X	0.99	142.960	2.09	Moderate
Imperial Valley-X	1.10	167.440	2.45	Moderate
Northridge-X	0.12	7.400	0.11	Slight
Northridge-X	0.25	19.490	0.29	Slight
Northridge-X	0.37	36.990	0.54	Slight
Northridge-X	0.50	55.320	0.81	Slight
Northridge-X	0.62	74.120	1.09	Moderate
Northridge-X	0.74	93.270	1.37	Moderate
Northridge-X	0.87	112.580	1.65	Moderate
Northridge-X	0.99	131.980	1.93	Moderate
Northridge-X	1.12	151.420	2.22	Moderate
Northridge-X	1.24	170.890	2.50	Moderate
Kobe-Y	0.11	3.040	0.04	Slight
Kobe-Y	0.22	4.500	0.07	Slight
Kobe-Y	0.34	5.380	0.08	Slight
Kobe-Y	0.45	6.150	0.09	Slight
Kobe-Y	0.56	7.660	0.11	Slight
Kobe-Y	0.67	9.760	0.14	Slight
Kobe-Y	0.78	12.830	0.19	Slight
Kobe-Y	0.90	15.920	0.23	Slight
Kobe-Y	1.01	18.990	0.28	Slight
Kobe-Y	1.12	22.070	0.32	Slight
Imperial Valley-Y	0.12	3.470	0.05	Slight
Imperial Valley-Y	0.24	4.770	0.07	Slight
Imperial Valley-Y	0.35	6.050	0.09	Slight
Imperial Valley-Y	0.47	7.010	0.10	Slight
Imperial Valley-Y	0.59	9.800	0.14	Slight
Imperial Valley-Y	0.71	12.360	0.18	Slight
Imperial Valley-Y	0.83	15.190	0.22	Slight
Imperial Valley-Y	0.94	18.200	0.27	Slight
Imperial Valley-Y	1.06	21.110	0.31	Slight
Imperial Valley-Y	1.18	23.800	0.35	Slight
Northridge-Y	0.15	2.890	0.04	Slight
Northridge-Y	0.31	5.570	0.08	Slight
Northridge-Y	0.46	8.690	0.13	Slight
Northridge-Y	0.62	11.630	0.17	Slight
Northridge-Y	0.77	14.480	0.21	Slight
Northridge-Y	0.92	17.230	0.25	Slight
Northridge-Y	1.08	9.950	0.29	Slight
Northridge-Y	1.23	22.670	0.33	Slight
Northridge-Y	1.39	25.360	0.37	Slight
Northridge-Y	1.54	28.050	0.41	Slight

Table 15 Bridge performance level

Description	Drift (%)
Operational (slight)	0 - 1
Life safety (moderate)	1 - 3
Near collapse (extensive)	3 - 5
Collapse (complete)	5 - 8.7

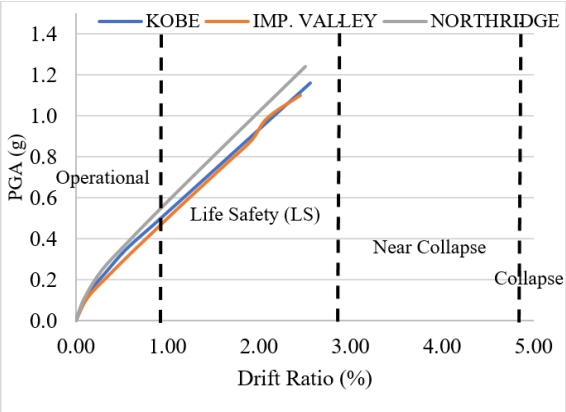

Fig. 6 Incremental Dynamic Analysis (IDA) curve

Table 16 Bridge damage and performance assessment

Dam level	Damage Classification	Damage Description (Damage Measures)	Perform. Level
I	No	• Onset of hairline cracks	Fully operational
II	Minor	• Crack widening • Theoretical first yield of longitudinal reinforcement	Operational
III	Moderate	• Initiation of inelastic deformation • Onset of cover concrete spalling • Development of diagonal cracks	Limited damage
IV	Major	• Formation of very wide cracks • Extended concrete spalling	Life safety
V	Local failure/ collapse	• Buckling of main reinforcement • Rupture of transverse reinforcement • Crushing of core concrete	Collapse

IDA curve aims to graphically represent how the probability of reaching or exceeding a certain level of structural damage changes with incremental increases in ground motion intensity or another relevant parameter. Based on the assessment of bridge damage and performance [11], the prestressed concrete bridge is classified with major damage and a life safety performance level, as shown in Table 16. This classification indicates the formation of very wide cracks and extended concrete spalling post-disaster earthquakes, as shown in Fig. 6.

4.2.2 Fragility curve

A fragility curve is a curve that displays the probability of structural damage due to earthquake loads with a certain intensity. Keith Porter formulates probability values [12], as follows Eq. (4):

$$P = \phi\left(\frac{\ln\left(\frac{x}{\theta}\right)}{\beta}\right) \quad (4)$$

where P is the probability of structural damage; ϕ is the standard normal function; x is ground motion parameter PGA (g); θ is median demand capacity PGA (g); β is the total uncertainly of the structure; v is the coefficient of variation of the damage limit; σ is standard deviation of the damage limit; μ is mean of the damage limit.

Table 17 illustrates the Peak Ground Acceleration (PGA) values intersecting the boundary line of structural damage. These values are utilized to determine the uncertainty of the structure and the median demand.

Table 17 PGA rated each damage limit

Earthquake Load	Slight PGA (g)	Moderate PGA (g)	Extensive PGA (g)	Complete PGA (g)
Kobe	0.519	1.353	2.186	3.729
Imperial Valley	0.495	1.351	2.208	3.792
Northridge	0.568	1.480	2.391	4.077

Table 18 Structural uncertainty

Type Earthquake	Slight PGA (g)	Moderate PGA (g)	Extensive PGA (g)	Complete PGA (g)
Kobe	0.519	1.353	2.186	3.729
Imperial Valley	0.495	1.351	2.208	3.792
Northridge	0.568	1.480	2.391	4.077
σ	0.037	0.074	0.113	0.186
μ	0.527	1.395	2.262	3.866
v	0.071	0.053	0.050	0.048
θ	0.526	1.393	2.259	3.862
β	0.071	0.053	0.050	0.048

Structural uncertainty (β) is obtained through the following Eq. (5):

$$\beta = \sqrt{\ln(1+v^2)} \quad (5)$$

Table 18 shows the calculation results of structural uncertainty. The median value of seismic demand (θ) is obtained through the following Eq. (6):

$$\theta = \frac{\mu}{\sqrt{1+v^2}} \quad (6)$$

Once all the constituent values of the probability of brittleness are obtained, calculations can be made for the fragility curve, as in Eq. (4).

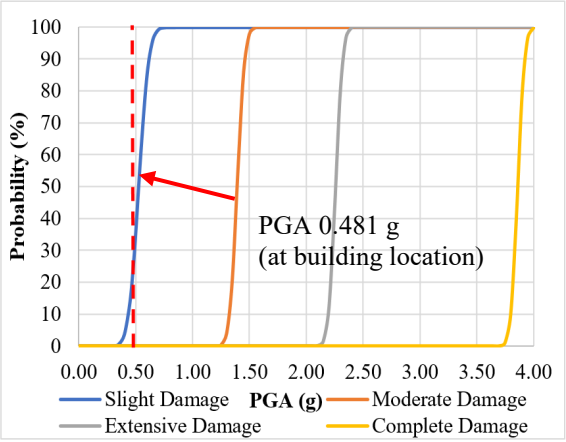

Fig. 7 Fragility curve of prestressed concrete bridge

The PGA value in Padang Pariaman, West Sumatra, the location of the prestressed concrete bridge based on the 2010 earthquake map and Indonesian bridge standard SNI 2833:2016 calculation, is 0.481g. Fig. 7 shows that PGA 0.481g has a 26% probability of experiencing slight damage; there is no possibility of moderate, extensive or complete damage, so the prestressed concrete bridge structure is resistant to loads that work according to current Indonesian bridge regulations.

5. CONCLUSION

The seismic performance of prestressed concrete bridge structures against earthquake loads was evaluated, and it can be concluded that the capacity and deflection of prestressed concrete bridges meet the permit limits, where the maximum moment, shear, and deflection values are smaller than the capacity and deflection values permitted by the current Indonesian bridge code.

In addition, the developed fragility curve shows that the prestressed concrete bridge STA 6+200, with a PGA in Padang Pariaman Regency value of 0.481g, has a 26% probability of experiencing slight damage. There is no possibility of moderate, extensive, or complete damage, so the prestressed concrete bridge structure is resistant to loads that work according to current Indonesian bridge regulations.

6. ACKNOWLEDGEMENTS

The authors gratefully acknowledge the financial support provided by Universitas Andalas.

7. REFERENCES

[1] Made S. and Anastasia M. S., Investigation of the Collapse of The Cincin Lama Bridge with Consideration of Fatigue Damage, International Journal of GEOMATE, Vol.26, Issue 115, 2024, pp. 100–107.

[2] Ko YY., Tsai CC., Hwang Y. W., Ge L., and Chu M. C, Failure of engineering structures and associated geotechnical problems during the 2022 ML 6.8 Chihshang earthquake, Taiwan. Nat Hazards, Vol. 118, 2023, pp. 55–94.

[3] Dang P. V., Huh J., Ahn JH, Haldar A., and Kwak K., Seismic Fragility Assessment for a Newly Developed Buried Arch Bridge, KSCE Civ Eng, Vol. 27, 2023, pp. 4849-4864.

[4] Hua L., Yongyan L., Jianqiang F., Bin L., Wenjuan L., Seismic Vulnerability Analysis of Long Span Prestressed Concrete Continuous Rigid Frame Bridge, Journal of Engineering Science and Technology, Vol. 15, Issue 6, 2022, pp. 35-41.

[5] Mondragón, Cortés C. M., Guerrero J. M. J., Navarrete B. A. O., and Ruiz G. M., Fragility Curves of RC Bridges in México, Applied Mechanics and Materials, Vol. 906, Trans Tech Publications, Ltd., 2022, pp. 75–80.

[6] Miluccio G., Losanno D., Parisi F., and Cosenza E., Fragility Analysis of Existing Prestressed Concrete Bridges Under Traffic Loads According to New Italian Guidelines, Structural Concrete, Vol. 24, 2023, pp. 1053-1069.

[7] CSI, Analysis Reference Manual for SAP2000, ETABS, and SAFE – Computers and Structures, Inc. Berkeley, California, USA, 2020.

[8] Indonesian National Standardization Agency, SNI 1725:2016 Loading for Bridges, BSN, Jakarta, 2016, pp.1-75.

[9] Indonesian National Standardization Agency, SNI 2833:2016 Earthquake Resistance Planning Standard for Bridges, BSN, Jakarta, 2016, pp.26-27.

[10] Federal Emergency Management Agency, HAZUS-MH MR4 Technical & User's Manual Multi-hazard Loss Estimation Methodology: Earthquake Model, 2003, pp. 143-144.

[11] Transportation Research Board, The National Academies National Cooperative Highway Reasearh Program (NCHRP) Synthesis 440, 2013, pp.40.

[12] Porter K., A Beginner's Guide to Fragility, Vulnerability, and Risk, 2021, pp. 2-9.